Available online at www.sciencedirect.com
ScienceDirect
Journal of the European Ceramic Society 29 (2009) 517–523
www.elsevier.com/locate/jeurceramsoc

Quantitative interpretation of the parabolic and nonparabolic oxidation behavior of nitride ceramic

X.-M. Hou, K.-C. Chou *

Metallurgical and Ecological Engineering School, University of Science and Technology Beijing, Beijing 100083, PR China

Received 14 April 2008; received in revised form 2 June 2008; accepted 20 June 2008

Abstract

The oxidation behavior of nitride ceramic under the conditions of different rate-controlling steps existing has been investigated from theoretical aspect. A series of formulae have been introduced to express the oxidation weight gain and oxide layer thickness as a function of temperature, time and the size of materials explicitly. They give an analytic solution, which simplifies the calculation and is convenient for theoretical analysis and discussion. Available experimental data in literature for oxidation of nitride ceramic were used to evaluate the model. Good agreement was obtained between theory and experimental data.

Keywords: Oxidation; Kinetics; Nitride ceramic

1. Introduction

Compared with oxide material, nitride materials posses good mechanical properties and have been widely developed in the past two decades as structural and functional ceramic. For example, silicon nitride (Si_3N_4) ceramic possesses excellent properties at both room temperature and high temperatures and has been used in the structural members of gas turbine, engines and other parts subjected to high-temperature conditions.[1–4] Silicon carbonitride (SiCN) ceramic is a potentially useful candidate for next generation high-temperature structural material because of its exceptional high-temperature creep resistance and thermal stability.[5,6] Aluminum nitride (AlN) finds wide applications as an electronic packing material, heat radiation fins and refractory materials, etc. because of its high thermal conductivity, excellent electrical resistivity and comparable coefficient of thermal expansion to silicon.[7–9] SiAlON-based ceramic is a general name for a large family of the so-called ceramic alloys based on silicon nitride. They have been developed actively since initially discovered in the early 1970s especially used as blast furnace refractories owing to their excellent high-temperature strength.[10]

In view of their wide application, the high-temperature chemical stability of these materials, especially their oxidation behavior, is one of the most important properties to be understood clearly before actual application. A lot of scientists have been researching the oxidation behavior of these materials using many techniques including X-ray diffraction, infrared spectroscopy, thermogravimetric analysis, X-ray photoelectron spectroscopy (XPS), scanning electron microscopy (SEM), and transmission electron microscopy (TEM), etc. However, because oxidation is affected by many parameters such as oxygen pressure, temperature and character of the sample, etc., there are wide variations, especially in the observed reaction rates, various kinetics models have been proposed. Take the oxidation of AlN for example, Kim and Moorhead reported that the oxidation kinetics of sintered aluminum nitride followed linear rate law while at higher temperature became parabolic.[11] Sato et al. found that at temperature of 1249.85 °C the oxidation kinetics of hot-pressed AlN, without additives, followed a parabolic rate law. This implies that the rate-controlling step in the oxidation of AlN is the diffusion of the oxidizing species through a protective oxide layer.[12] Same problems also exist in oxidation of other nitride materials.

As mentioned above, because of the variety of oxidation conditions, discussion and comparison of these oxidation data directly is impossible. Although there are some models in literature, such as the well known Jander model,[13] describing

* Corresponding author. Tel.: +86 10 6233 2646; fax: +86 10 6233 2570.
E-mail address: kcc126@126.com (K.-C. Chou).

0955-2219/$ – see front matter © 2008 Elsevier Ltd. All rights reserved.
doi:10.1016/j.jeurceramsoc.2008.06.015

the oxidation behavior, while its expression is not an explicit function of the oxidation fraction ξ and time t, oxygen partial pressure P_{O_2} and particle size, etc. It is not convenient for practical application. Other models reported in literature, such as the model offered by Persson and Nygren,[14] however, turn to many complicated mathematic treatments and get an implicit solution. Therefore, they cannot be accepted by most of the researchers. Thus far, the understanding of the oxidation behavior of the nitride material has been primarily qualitative. For engineering application, a theoretical quantitative description for oxidation process is required. In our previous paper,[15,16] we have developed a method to find an analytic solution to express the oxidation fraction ξ as an explicit function of time t, oxygen partial pressure P_{O_2}, particle size R_0 or pellet size H_0 under some approximate but reasonable assumptions. This method works well but it is only suitable for the case where oxygen diffusion in the oxide layer is the controlling step. Nevertheless, in some cases of oxidation reaction, the controlling step is not limited in oxygen diffusion. Various kinds of situations are possible. Therefore, the long-term objective of this work is to develop a model that can describe the oxidation behavior where all kinds of possible controlling steps exist. Since the formula are all analytic solutions expressing the relationships of the reacted fraction of oxidation ξ with time t, temperature T and other variables, they are not only easy to use but also can predict the effect of various factors such as temperature T and time t on oxidation behavior. This model gives a good theoretical guidance to nitride materials.

2. Mechanism of oxidation reaction and the expression of reaction rate for various kinds of steps

A general mechanism of oxidation reaction for pellet can be described as the following steps, they are:

(i) Oxygen in the bulk gas phase transfer to the surface of nitride ceramic.
(ii) Oxygen diffusion through the boundary layer between gas phase and solid phase.
(iii) Physisorption of oxygen molecules.
(iv) Dissociation of oxygen molecules and chemisorption.
(v) Surface penetration of oxygen atoms.
(vi) Diffusion of oxygen through the oxide product layer to the oxide/nitride interface.
(vii) Nucleus formation and chemical reaction producing oxide product and gas.
(viii) Gas diffusion through oxide product to the surface of nitride ceramic.
(ix) Gas diffusion through the gas/pellet boundary to the gas bulk.

Of course, if needed, one may give more intermediate steps, however, the above nine steps are basically enough to describe this kind of mechanism. In most cases, the steps (vi) and (vii) will be the rate-controlling step. It is because the chemical reaction and the diffusion of oxygen through oxide layer are slower. At present let us mainly treat oxidation kinetics under these two cases. Fig. 1 shows a schematic diagram of mechanism of oxidation between oxygen and nitride material (α). The shape of nitride material is cuboid with the size of $M_0 \times L_0 \times H_0$ (M_0, L_0 and H_0 represent length, width and height, respectively). When this cuboid is placed on a backstop and exposed to oxygen atmosphere, the five faces of it would react with oxygen to produce a oxide layer (β represents oxide phase with thickness of x). To proceed to the oxidation reaction continuously, the oxygen in the surface will get into the inner of cuboid through diffusion and react with substance materials to generate oxide. However, the complex oxidation mechanism makes it necessary to start with a model for simpler systems and conditions, where reliable and well-defined experimental data are available. According to experimental results in literature,[6,14,17,19] the height, H_0, is usually much smaller. Thus the oxidation of the four sides of the cuboid can be neglected. Based on this, the oxidation model can be simplified as shown in Fig. 2, in which, α represents nitride with thickness of H_0, β is oxide layer with thickness of x. Based on this, the formulae of oxidation of pellet can be derived as follows. A more comprehensive treatment when the height, H_0, cannot be ignored will be done and the results will be reported in another paper.

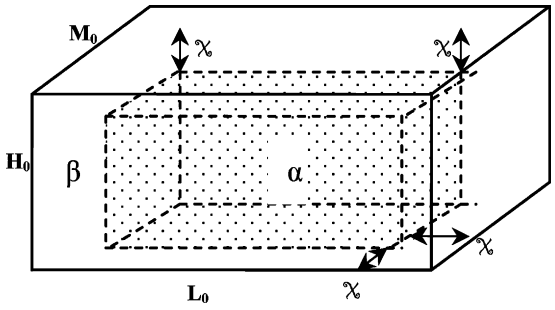

Fig. 1. A schematic diagram of mechanism of oxidation between oxygen and nitride material.

The transferred (or reacted) fraction of oxide ξ at thickness x and time t can be calculated in the light of the following equation:

$$\xi = \left(\frac{x}{H_0}\right) \tag{1}$$

Differentiating Eq. (1) with respect to time t, one obtains,

$$\frac{d\xi}{dt} = \frac{1}{H_0}\frac{dx}{dt} \tag{2}$$

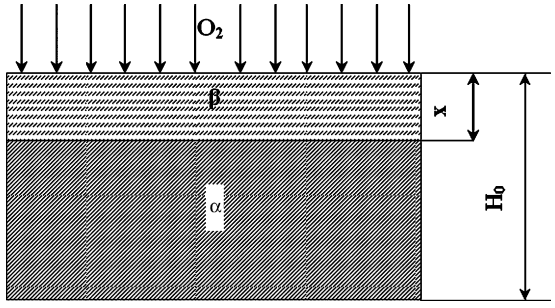

Fig. 2. Schematic plot of the oxidation of a pellet in an oxygen environment.

On the other hand, the time derivative of thickness x is proportional to the rate of oxidation reaction, i.e.,

$$\frac{dx}{dt} = \frac{V}{v_m} \tag{3}$$

where V is the reaction rate and v_m is a coefficient that is related to the density of reactant and product. Combining Eqs. (1)–(3) and rearranging it, one obtains

$$\frac{d\xi}{dt} = \frac{1}{H_0}\frac{V}{v_m} \tag{4}$$

Substituting different kinds of reaction rate at various controlling steps in Eq. (4), one may find the expressions of the reacted fractionξ and time t, integrating Eq. (4) with the initial condition, $t=0$, $\xi=0$, one obtains

$$\xi = \frac{1}{H_0}\frac{V}{v_m}t \tag{5}$$

2.1. Diffusion of oxygen in oxide

2.1.1. Derivation of formulae

According to Fick's diffusion law, the diffusion rate of oxygen V in the β phase can be expressed as

$$V = J_O^\beta = -D_O^\beta\left(\frac{C''^\beta_O - C'^\beta_O}{x}\right) \tag{6}$$

where J_O^β, D_O^β and C_O^β represent the flux, diffusion coefficient and concentration of oxygen in β phase, respectively. x is the distance along the direction of oxygen flux, i.e., the distance from the surface of gas/oxide to the interface of α/β (Fig. 2). C'^β_O, the concentration of oxygen in the β phase at the gas/β side and C''^β_O, the concentration of oxygen in the β phase at the α/β side. They will keep constant when the reaction is in a steady state.

Combining Eqs. (4) and (6) yields

$$\frac{d\xi}{dt} = -\frac{D_O^\beta(C''^\beta_O - C'^\beta_O)}{H_0^2 v_m \xi} \tag{7}$$

where v_m is a coefficient that is related to the density of reactant and product. Integrating the above equation with the initial condition of $\xi=0$ when $t=0$, we obtain

$$\xi = \sqrt{\frac{2D_O^\beta(C'^\beta_O - C''^\beta_O)}{H_0^2 v_m}t} \tag{8}$$

C'^β_O is in equilibrium with oxygen partial pressure in the bulk gas phase, which can be expressed as

$$C'^\beta_O = K\sqrt{P_{O_2}} \tag{9}$$

where K is an equilibrium constant. C''^β_O is also in equilibrium with oxide.

It is well known that the effect of temperature T on diffusion coefficient D_O^β obeys the Arrhenius law, i.e.,

$$D_O^\beta = D_O^{0\beta}\exp\left(-\frac{\Delta\varepsilon_d}{RT}\right) \tag{10}$$

Since K is the equilibrium constant for the reaction of oxygen gas dissolving into the oxide (β phase). This is a thermodynamic property, the relation of which with temperature can be expressed as

$$K = K_O^{0\beta}\exp\left(-\frac{\Delta H}{RT}\right) \tag{11}$$

Combining Eqs. (8)–(11) yields

$$\xi = \sqrt{\left(\frac{2K_O^{0\beta}D_O^{0\beta}}{v_m}\frac{\left(\sqrt{P_{O_2}}-\sqrt{P_{O_2}^{eq}}\right)}{H_0^2}\exp\left(-\frac{\Delta\varepsilon_d+\Delta H}{RT}\right)\right)t} \tag{12}$$

$$\text{define}\quad \Theta_T = \frac{v_m H_0^2}{2K_O^{0\beta}D_O^{0\beta}\left(\sqrt{P_{O_2}}-\sqrt{P_{O_2}^{eq}}\right)} \tag{13}$$

Eq. (12) becomes

$$\xi = \sqrt{\frac{1}{\Theta_T}\exp\left(-\frac{\Delta\varepsilon_d+\Delta H}{RT}\right)t} \tag{14}$$

Here we define the apparent activation energy as

$$\Delta E = \Delta\varepsilon_d + \Delta H \tag{15}$$

Thus we have

$$\xi = \sqrt{\frac{1}{\Theta_T}\exp\left(-\frac{\Delta E}{RT}\right)t} \tag{16}$$

It means that the calculated energy based on the above equation is apparent activation energy not normal activation energy.

2.1.2. Effect of T, P_{O_2} and H_0 on oxidation

From Eq. (16), we can see only the parameter Θ_T is related to the factors such as temperature T, oxygen partial pressure P_{O_2} and pellet size H_0. Therefore, it might be the starting point to derive the formulae describing the influence of temperature T, oxygen partial pressure P_{O_2} and pellet size H_0 on oxidation.

$$\text{Define}\quad \Theta = \frac{v_m}{2K_O^{0\beta}D_O^{0\beta}} \tag{17}$$

Substituting Eq. (17) into Eq. (12) yields

$$\xi = \sqrt{\left(\frac{1}{\Theta}\frac{\left(\sqrt{P_{O_2}}-\sqrt{P_{O_2}^{eq}}\right)}{H_0^2}\exp\left(-\frac{\Delta E}{RT}\right)\right)t} \tag{18}$$

This is the formula describing the effect of temperature T, oxygen partial pressure P_{O_2} and pellet size H_0 on oxidation under the controlling step of oxygen diffusion in oxide.

2.2. Chemical reaction

2.2.1. Derivation of formulae

For a chemical reaction, the oxidation reaction between oxygen and nitride material can be described as

$$\mathrm{O}(\alpha/\beta) + \mathrm{M}(\alpha) \underset{K_r^b}{\overset{K_r^f}{\rightleftarrows}} \mathrm{MO}(\alpha/\beta) + \mathrm{N} \tag{19}$$

The chemical reaction rate for forward V_r^f and backward V_r^b as well as the total reaction rate V_r, can be expressed as

$$V_r^f = K_r^f C_O(\beta/\alpha) \tag{20}$$

$$V_r^b = K_r^b C_N(\beta/\alpha) \tag{21}$$

$$V_r = V_r^f - V_r^b = K_r^f C_O(\beta/\alpha) - K_r^b C_N(\beta/\alpha) \approx K_r^f C_O(\beta/\alpha) - K_r^b C_N^{eq}(\beta/\alpha) \tag{22}$$

Since the equilibrium constant K_r for the reaction (19) is equal to

$$K_r = \frac{K_r^f}{K_r^b} = \frac{C_N^{eq}}{C_O^{eq}} \tag{23}$$

where C_O^{eq} and C_N^{eq} represents the equilibrium composition of oxygen and nitrogen in oxide as oxidation reaction reaches equilibrium, respectively, thus,

$$V_r = V_r^f - V_r^b = K_r^f C_O - K_r^f C_O^{eq} = K_r^f (C_O - C_O^{eq}) \tag{24}$$

Combining Eqs. (5), (9) and (24) yields

$$\xi = \frac{k_0}{v_m H_0}\left(\sqrt{P_{O_2}} - \sqrt{P_{O_2}^{eq}}\right)\exp\left(-\frac{\Delta E}{RT}\right)t \tag{25}$$

where

$$k_0 = k_O^{0r} K_O^{0\beta}; \qquad \Delta E = \Delta\varepsilon_r + \Delta H$$

$$\text{Define} \quad B_T = \frac{v_m H_0}{k_0\left(\sqrt{P_{O_2}} - \sqrt{P_{O_2}^{eq}}\right)} \tag{26}$$

Substituting Eq. (26) into Eq. (25) yields

$$\xi = \frac{1}{B_T}\exp\left(-\frac{\Delta E}{RT}\right)t \tag{27}$$

2.2.2. Effect of T, P_{O_2} and H_0 on oxidation

In an analogical way, the formula describing the influence of temperature T, oxygen partial pressure P_{O_2} and pellet size H_0 on oxidation is as follows:

$$\text{Define} \quad B = \frac{v_m}{K_0} \tag{28}$$

$$\xi = \frac{1}{BH_0}\left(\sqrt{P_{O_2}} - \sqrt{P_{O_2}^{eq}}\right)\exp\left(-\frac{\Delta E}{RT}\right)t \tag{29}$$

This is the formula describing the effect of temperature T, oxygen partial pressure P_{O_2} and pellet size H_0 on oxidation under the controlling step of chemical reaction. How accuracy of this kind of treatment can be judged from the application of this model to the practical examples that would be given in the latter sections.

3. Validity of the new model

In this section, the model was testified by the experimental data of oxidation of Si_3N_4 ceramic synthesized from chemical vapor deposition (CVD) method,[17] fully dense SiCN ceramic,[6] β-SiAlON ceramic with various z value[14] and AlN ceramic.[19] Their oxidation behaviors with all kinds of possible controlling steps are quantitatively investigated.

3.1. Diffusion-controlled reaction

3.1.1. Si_3N_4 ceramic synthesized from chemical vapor deposition (CVD) method

Ogbuji et al. had studied the oxidation kinetics of CVD Si_3N_4 from 1199.85 to 1499.85 °C with 100 °C intervals in 1 atm oxygen.[17] The experiment was carried out in quartz tubes to ensure a clean oxidation environment because it had been reported that impurities in alumina tubes influenced both the oxidation kinetics and the oxide scale phase and microstructure.[18] The size of the samples were cut into 8 mm × 5 mm × 1 mm and the oxidation time was 5 h (18,000 s), 10 h (36,000 s), 25 h (90,000 s), 50 h (180,000 s), 75 h (270,000 s) and 100 h (360,000 s), respectively. After oxidation, the microstructure and the oxide thickness were measured, respectively. The oxidation behavior at different temperature is shown in Fig. 2. The experiment showed that the oxidation rate was limited by permeation of oxygen through oxide layer and the oxidation activation energy was determined to be 363 kJ/mol. At present, let us use our model to fit these data. According to Eq. (16), there are two parameters Θ_T and ΔE that are required to be determined by fitting the experimental data. Based on the experimental data, these two parameters are easily extracted by regression to be 325.56 kJ/mol and 8.5, respectively. Substituting the above ΔE and Θ_T data into Eq. (16), the model describing isothermal oxidation behavior of Si_3N_4 is as follows:

$$\zeta = 0.343\sqrt{t}\,\exp\left(-\frac{19518.9}{T}\right) \tag{30}$$

For comparison the theoretical predicted lines are also presented in Fig. 3. It may be seen that the experimental data and theoretical prediction are in good agreement, validating the present theoretical approach. Please note that, the ordinate of Fig. 3 is using thickness ζ in stead of reacted fraction ξ. We should make a transformation when using Eq. (16). Eq. (30) can also predict the oxidation behavior of Si_3N_4 within the same oxidation mechanism. The black lines of 1349.85 and 1449.85 °C in Fig. 3 are completely theoretical predicted based on our limited information.

3.1.2. Fully dense SiCN ceramic

Fig. 4 shows a typical plot of oxide thickness (mm) vs. oxidation time (s) for SiCN ceramic pellet in air at temperatures of 899.85 °C, 999.85 °C, 1099.85 °C and 1199.85 °C for

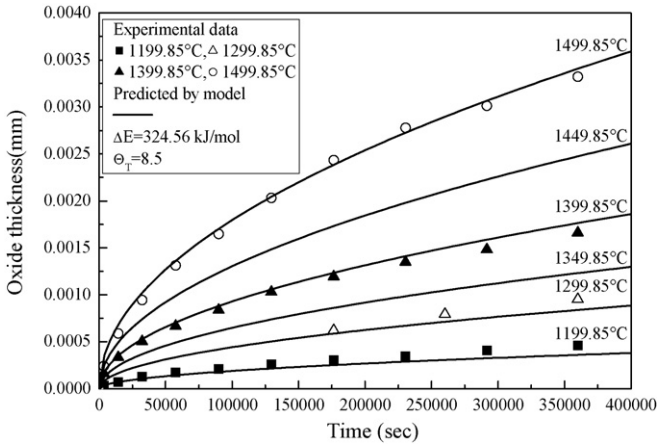

Fig. 3. A comparison of plots from diffusion-controlled model and experimental data for isothermal oxidation of CVD Si_3N_4 in 1 atm oxygen.

20 h (180,000 s), 50 h (180,000 s), 100 h (360,000 s) and 200 h (720,000 s) each.[6] The size of the samples was 12.7 mm in diameter and 2–3 mm in thickness. The oxide thickness was measured using SEM. The experimental results showed that the oxide layer fitted a typical parabolic kinetics and the calculated activation energy was 120 kJ/mol. Similarly, we apply Eq. (16) to fit the experimental data and the results are also shown in the same figure for comparison. We can see that the theoretical results and the experimental data reach a good agreement. In addition, the oxidation behavior at 949.85, 1049.85 and 1149.85 °C is also completely predicted using Eq. (31) (shown in Fig. 4)

$$\zeta = 0.0032\sqrt{t}\ \exp\left(-\frac{7213.74}{T}\right) \tag{31}$$

3.1.3. β-SiAlON ceramics

Persson and Nygren comprehensively researched the oxidation behavior of single β-SiAlON ($Si_{6-z}Al_zO_zN_{8-z}$) ceramic with z values of 0.5, 1, 2.5 and 3.8.[14] Pieces of an approximate 15 mm × 5 mm × 1 mm size were used for the oxidation experiments. The samples were oxidized isothermally in flowing oxygen for 20 h at the temperatures ranging from 1199.85 to 1449.85 °C in the TG unit SETARAM TAG 24. Fig. 5a and b are oxidation results for β-SiAlON ($Si_{6-z}Al_zO_zN_{8-z}$) ceramic with z values of 2.5 and 3.8 prepared with Si_3N_4 powder from UBE (Japan, grade SN-10E). It revealed that both β-SiAlON ceramic with z value of 2.5 and 3.8 fitted parabolic rate law. While β-SiAlON ceramic with z value of 3.8 was more oxidation resistant. We also apply Eq. (16) to describe their oxidation behavior and their equations are as follows:

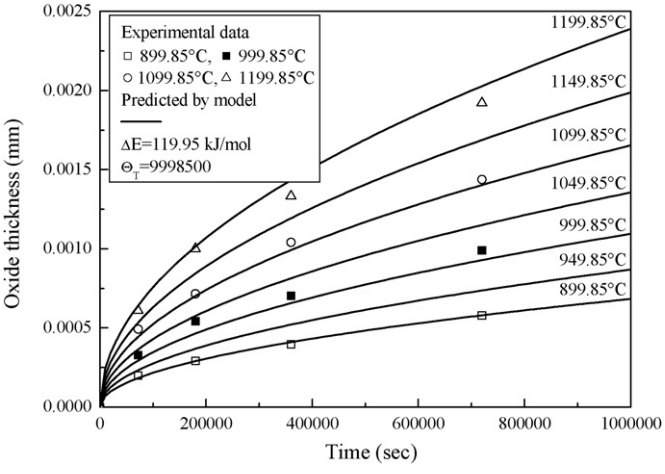

Fig. 4. A comparison of plots from diffusion-controlled model and experimental data for isothermal oxidation of fully dense SiCN.

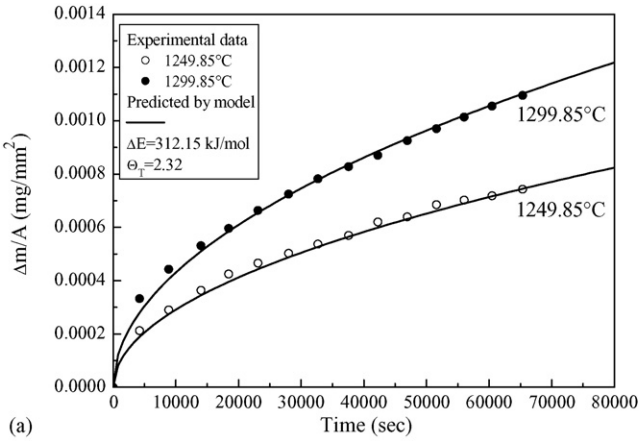

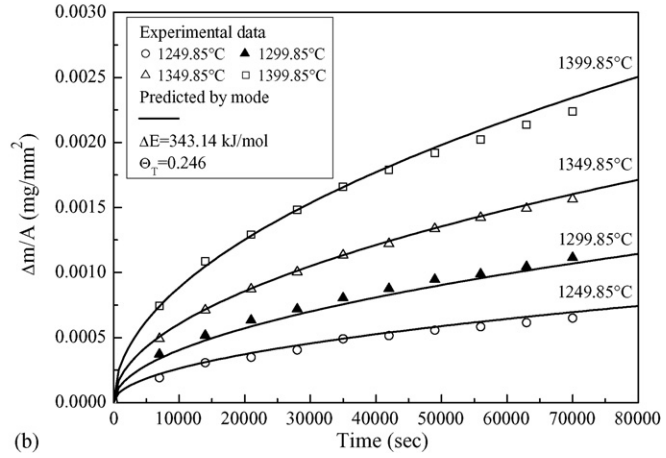

Fig. 5. A comparison of plots from diffusion-controlled model and experimental data for isothermal oxidation of β-SiAlON ceramic with various z value. (a) $z = 2.5$ and (b) $z = 3.8$.

β-SiAlON ceramic with z value of 2.5

$$\zeta = 0.657\sqrt{t}\ \exp\left(-\frac{18772.55}{T}\right) \tag{32}$$

β-SiAlON ceramic with z value of 3.8

$$\zeta = 2.015\sqrt{t}\ \exp\left(-\frac{20636.5}{T}\right) \tag{33}$$

The lines calculated from the above equations are shown in the same figure (Fig. 5a and b). It can be seen that the equations fit the experimental data very well. In addition, the oxidation activation energy obtained from the equations showed that β-SiAlON ceramic with z values of 3.8 possesses higher value (343.14 kJ/mol) than that of β-SiAlON ceramic with z values of

Table 1
Comparison of oxidation parameters calculated by the new model and reported in literature

Sample	ΔE (kJ/mol)	
	Calculated from the new model	Reported in literature
Si_3N_4 ceramic (CVD)	324.56	363 (offered by Ogbuji et al.)
SiCN ceramic	119.95	120 (offered by Bharadwaj et al.)
β-SiAlON ceramic ($z = 2.5$)	312.15	330 (offered by Persson and Nygren)
β-SiAlON ceramic ($z = 3.8$)	343.14	360 (offered by Persson and Nygren)
AlN ceramic	243.85	233 (offered by Xu et al.)

2.5 (312.15 kJ/mol). This could explain the experimental fact that β-SiAlON ceramic with z value of 3.8 is more oxidation resistant.

3.2. Chemical reaction

The effects of atmosphere and humidity on the oxidation behavior of AlN ceramic were investigated by Xu et al.[19] The results showed that the oxidation behavior was greatly affected by the humidity and the oxidation in dry air followed a linear rate law between 1099.85 and 1299.85 °C with the apparent activation energy of 233 kJ/mol (Fig. 6). Here, we use Eq. (27) to describe the oxidation behavior at 1199.85 and 1299.85 °C, respectively and the equation is as follows:

$$\frac{\Delta m}{A} = 649.4x \exp\left(-\frac{29330.1}{T}\right) \tag{34}$$

The results calculated from the above equation are shown in the same figure and also get a very good agreement.

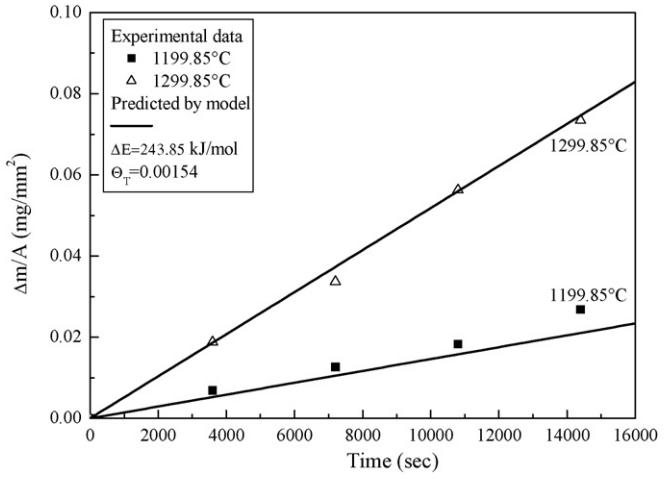

Fig. 6. A comparison of plots from chemical reaction-controlled model and experimental data for isothermal oxidation of AlN ceramic.

4. Parametric reliability studies

It is well known that the activation energy, ΔE, is a very useful parameter to evaluate the property of oxidation resistance of nitride materials. The value of ΔE calculated from our new model and reported in literature is summarized in Table 1 for comparison.

From the table, we can see that some deviation exists between the results obtained from the new model and the literature. This is possibly caused by the mathematical calculation when we use these models. We can directly obtain the value by regression method when using the new model. While the models used by many researchers, such as, Jander model, need many times of regression to get the value since its expression is not an explicit function. This will possibly cause larger errors. Therefore, as viewed from mathematical treatment, the value of ΔE obtained from our new model is more precise than that using the traditional models.

A series of equations for oxidation under the conditions where all kinds of possible controlling steps exist have been developed. They quantitatively express the relation of the reacted fraction of oxidation with various variables, such as time t, temperature T, oxygen partial pressure P_{O_2}, pellet size H_0, etc. They are all explicit analytic function. Therefore, it is convenient to be used as a tool of theoretical analysis.

Besides describing the oxidation behavior reasonably, the new model can also predict the oxidation behavior within the same oxidation mechanism using limited experimental data. The curves of 1349.85 and 1449.85 °C in Fig. 3 and 949.85, 1049.85 and 1149.85 °C in Fig. 4 are completely predicted by the new model.

In the derivation of our formulae, the variable used is the "reacted fraction" or "transferred fraction", ξ; however, many researchers prefer to use the variables "increment of the reaction", Δm, or "thickness of oxide layer", ζ, instead of ξ. We can carry out a transformation of the variables prior to using the formulae since there exists a proportional relation between the variables. In addition, the application of this new model actually is not limited in the treatment of the oxidation of nitride materials, but in dealing with problems of other materials, such as the kinetics of hydriding/dehydriding reactions in alloys[20] because these equations are the general form in dealing with the solid–gas reaction. Therefore, it should have a more promising future in the material field.

5. Conclusion

Systematic formulae concerning the oxidation behavior of nitride materials where various kinds of rate-controlling steps exist have been presented in our work. These formulae express the reacted fraction of oxidation ξ, oxide thickness ζ, or oxidation mass increment Δm as an explicit function of time t,

temperature T, oxygen partial pressure P_{O_2} and pellet thickness L_0. They are greatly convenient for both calculation and discussion. The application of the new model to the practical system shows that it is feasible. The new model can also predict the oxidation behavior within the same reaction mechanism. Since most of oxidation processes of inorganic non-metallic materials had very similar mechanism, it might be expected that this new model would be suitable for the oxidation process of many other inorganic non-metallic systems.

Acknowledgements

The authors would like to express their thanks to the Science and Technology Committee of Shanghai for their kind support on contract no. 0452NM002. The authors would also like to express their thanks to Ogbuji et al., Bharadwaj et al., Persson et al. and Xu et al. for their kind offering of experimental data.

Appendix A. Nomenclature

C_O^{eq}	the equilibrium composition of oxygen in oxide
C_N^{eq}	the equilibrium composition of nitrogen in oxide
$D_O^{0\beta}$	diffusion coefficient of oxygen in oxide phase
ΔE	apparent activation energy of oxidation
H_0	height of the cuboid of nitride material
K_r	equilibrium constant
$K_O^{0\beta}$	reaction equilibrium constant coefficient
L_0	width of the cuboid of nitride material
Δm	the increment of sample weight
M_0	length of the cuboid of nitride material
P_{O_2}	partial pressure of oxygen in gas phase
$P_{O_2}^{eq}$	oxygen partial pressure in equilibrium with oxide
R	gas constant
t	time in s
T	absolute temperature with K
v_m	a coefficient that is related to the density of reactant and product
x	the thickness of oxide layer

Greek symbols

α	original nitride material
β	nitride material after oxidation
ζ	thickness of the oxide layer
ξ	reacted fraction of oxidation

References

1. Sheeham, J. E., Passive and active oxidation of hot-pressed silicon nitride materials with two magnesia contents. *J. Am. Ceram. Soc.*, 1982, **65**(7), C111–C113.
2. Riley, F. L., Silicon nitride and related materials. *J. Am. Ceram. Soc.*, 2000, **83**(2), 245–265.
3. Lange, F. F., The sophistication of ceramic science through silicon nitride studies. *J. Ceram. Soc. Jpn.*, 2006, **114**(11), 873–879.
4. Ogata, S., Hirosaki, N., Kocer, C. and Shibutani, Y., A comparative ab initio study of the 'ideal' strength of single crystal α- and β-Si_3N_4. *Acta Mater.*, 2004, **52**, 233–238.
5. Raj, R., An, L. N., Shah, S., Riedel, R., Fasel, C. and Kleebe, H. J., Oxidation kinetics of an amorphous silicon carbonitride ceramic. *J. Am. Ceram. Soc.*, 2001, **84**(8), 1803–1810.
6. Bharadwaj, L., Fan, Y., Zhang, L. G., Jiang, D. P. and An, L. N., Oxidation behavior of a fully dense polymer-derived amorphous silicon carbonitride ceramic. *J. Am. Ceram. Soc.*, 2004, **87**(3), 483–486.
7. Luo, B., Johnson, J. W., Kryliouk, O., Ren, F., Pearton, S. J., Chu, S. N. G., Nikolaev, A. E., Melnik, Y. V., Dmitriev, V. A. and Anderson, T. J., High breakdown M–I–W structures on bulk AlN. *Solid State Electron.*, 2002, **46**, 573–576.
8. Slack, G. A., Nonmetallic crystals with high thermal conductivity. *J. Phys. Chem. Solids*, 1973, **34**, 321–325.
9. Strite, S. and Morkoc, H., Gallium nitride, aluminum nitride and indium nitride: a review. *J. Vac. Sci. Technol. B*, 1992, **10**, 1237–1266.
10. Jack, K. H. and Wilson, W. I., Ceramics based on the Si–Al–O–N and related systems. *Nat. Phys. Sci. (Lond.)*, 1972, **238**, 28–29.
11. Kim, H.-E. and Moorhead, A. J., Oxidation behavior and flexural strength of aluminum nitride exposed to air at elevated temperatures. *J. Am. Ceram. Soc.*, 1994, **77**(4), 1037–1041.
12. Sato, T., Haryu, K., Endo, T. and Shimada, M., High temperature oxidation of hot-pressed aluminum nitride by water vapor. *J. Mater. Sci.*, 1987, **22**, 2277–2280.
13. Jander, W., Reactions in the solid state at high temperatures. *Z. Anorg. U. Allgem. Chem.*, 1927, **163**(1–2), 1–30.
14. Persson, J. and Nygren, M., The oxidation kinetics of β-SiAlON ceramics. *J. Eur. Ceram. Soc.*, 1994, **13**(5), 467–484.
15. Chou, K. C., A kinetics model for oxidation of Si–Al–O–N materials. *J. Am. Ceram. Soc.*, 2006, **89**(5), 1568–1576.
16. Hou, X. M., Chou, K. C. and Li, F. S., Some new perspectives on oxidation kinetics of SiAlON materials. *J. Eur. Ceram. Soc.*, 2008, **28**, 1243–1249.
17. Ogbuji, L. U. J. T. and Opila, E. J., A comparison of the oxidation kinetics of SiC and Si_3N_4. *J. Electrochem. Soc.*, 1995, **142**(3), 925–930.
18. Zheng, Z., Tressler, R. E. and Spear, K. E., Effect of sodium contamination on the oxidation of single crystal carbide. *Corros. Sci.*, 1992, **33**(4), 569–580.
19. Xu, X. R., Yan, W. L., Zhuang, H. R., Li, W. L. and Xu, S. Y., Oxidation behavior of aluminum nitride. *J. Inorg. Mater.*, 2003, **18**(2), 337–342.
20. Chou, K. C., Li, Q., Lin, Q., Jiang, L. J. and Xu, K. D., Kinetics of absorption and desorption of hydrogen in alloy powder. *Int. J. Hydrogen Energy*, 2005, **30**(3), 301–309.